JOURNAL OF MATERIALS SCIENCE **37** (2002) 5327–5331

The effect of composition on spinel equilibrium and crystal size in high-level waste glass

B. K. WILSON, P. HRMA, J. ALTON, T. J. PLAISTED, J. D. VIENNA
Pacific Northwest National Laboratory, Richland, Washington, USA
E-mail: pavel.hrma@pnl.gov

The equilibrium concentration (C_o) of spinel was measured in 16 high-level waste (HLW) glasses as a function of temperature (T). Glasses were formulated by increasing or decreasing concentrations of Al_2O_3, Cr_2O_3, Fe_2O_3, Li_2O, MgO, Na_2O, or NiO, one-at-a-time, from a baseline composition. Data were fitted using the quasi-ideal-solution relationship between C_o and T. The coefficients of this relationship were expressed as functions of glass composition using first-order approximation. All glass components had an effect on liquidus temperature (T_L), but only NiO and Fe_2O_3 had a significant impact on spinel concentration below T_L. The temperature at which C_o had a given value was also expressed as a function of glass composition. These results can be used to optimize a HLW glass formulation to meet a constraint of either no spinel or a limited spinel fraction in the melter. In addition, the measurement of the size of spinel crystals and subsequent calculation of crystal number density (n) showed that Cr_2O_4 and Al_2O_3 increase n.

1. Introduction

In the vitrification of high-level waste (HLW), efficiency relies on loading glass with as much waste as possible. Typically, glasses are formulated to assure that no crystals precipitate that are potentially harmful to the melter. The crystalline phase most likely to form in a Hanford HLW glass melter is spinel, a solid solution of trevorite, nichromite, and magnetite [1]. Precipitated spinel settles to form sludge on the bottom of the melter and thus decrease its usable life. Therefore, it is important that spinel formation is controlled to balance operational cost and potential risk to the melter.

The waste loading in glass is limited by the level of spinel that a melter can tolerate. This depends upon the rate at which the crystals settle and form sludge at the melter bottom. By reducing average crystal size, crystals settle at a lower rate. The composition of glass, especially the presence of nucleation agents, can greatly affect the spinel number density and the average crystal size [2].

To help determine the level of spinel a melter can tolerate, we measured the effect of glass composition and temperature on spinel precipitation below liquidus temperature (T_L). This includes finding the equilibrium mass fraction of spinel as a function of temperature below T_L. Also, we measured the size of spinel crystals that form as glass temperature drops below T_L.

2. Theory

At a temperature below T_L, the equilibrium compositions of spinel and glass and the equilibrium mass fraction of spinel (C_o) are related through the mass-balance equation, i.e., [3],

$$C_{r,i} = \frac{C_i - C_o C_{c,i}}{1 - C_o} \tag{1}$$

where $C_{r,i}$ is the i-th component mass fraction in residual glass and $C_{c,i}$ is the i-th component mass fraction in the crystalline phase.

If the primary phase is the only solid that precipitates, a temperature below T_L is the T_L of the residual glass (T_{Lr}) at equilibrium with the primary phase. Within the composition region of Hanford HLW glasses, the T_L can be described as a first-order function of the glass composition vector (**g**) [4, 5]. Hence [3, 6],

$$C_o = \frac{T_L - T}{\Theta - T} \tag{2}$$

where Θ is a function of spinel composition that may vary from approximately 2900 K to 15900 K [3]. The usefulness of Equation 2 is limited by the difficulty in determining spinel composition, and, thus, the value of Θ, with a sufficient accuracy. In this work, we used the

following empirical relationship between C_o and T to fit experimental data [7, 8]

$$C_o = C_{\max}\left\{1 - \exp\left[-B_L\left(\frac{1}{T} - \frac{1}{T_L}\right)\right]\right\} \quad (3)$$

where $C_{\max}$ and B_L are composition-dependant coefficients. $C_{\max}$ represents the hypothetical maximum fraction of crystalline phase as $T \to 0$ and B_L would be $\Delta H_d/R$, where ΔH_d is the dissolution enthalpy (which is assumed to be independent of T for small undercoolings), and R is the gas constant (ΔH_d is *not* a spinel heat of fusion). It is fortuitous that Equation 3 has the form of phase equilibrium in a binary ideal solution. Other shapes of C_o vs. T curves were obtained for spinel in glasses within different composition regions [9].

Rearranging Equation 3 to express T as a function of C_o, developing the resulting relationship into a truncated Taylor series, and denoting $T_L - T = \Delta T$, we obtain

$$\Delta T = \frac{C_o T_L^2}{C_{\max} B_L} \quad (4)$$

This equation is valid if $C_o/C_{\max} \ll 1$.

Glass properties are functions of glass composition. In the neighborhood of a baseline composition, these functions can be approximated as first-order polynomials (this approximation has been widely used in the literature—see, for example, Scholze [10]). Accordingly,

$$\phi = \sum_{i=1}^{N} \phi_i g_i \quad (5)$$

where Φ_i is the i-th component coefficient (the partial specific property) for property Φ, g_i is the i-th component mass fraction in glass, and N is the number of components. Equation 5 applies to $\Phi = (C_{\max}, B_L, T_L, \Delta T, a, n)$, where a is the average crystal size and n is the spinel number density.

3. Experimental

We chose MS-7 glass [2] as the baseline and formulated 15 experimental glasses by increasing or decreasing the concentrations of seven different components (Al, Cr, Fe, Li, Mg, Na, and Ni), one-at-a-time, from the baseline composition (Table I). All components, except those that were varied, remained at the same proportions as in the baseline glass.

The batches were prepared by mixing reagent grade or better oxides, carbonates, and boric acid, and melting them in a covered Pt-5%Rh crucible at 1250°C (expect VH-Ni, which was melted at 1300°C) for 1 h. The glasses were quenched by pouring the melts on a clean steel plate and were then crushed in a tungsten-carbide mill for 5 min, remelted under the same conditions, and quenched again in the same manner. Glass samples were heat treated in approximately 1-mL Pt-5%Au crucibles placed either in a uniform or gradient-temperature furnace, and quenched in air. Heat-treatment temperatures varied from 700°C to 1250°C. Based on previous studies, heat-treatment times (3 h to 72 h, depending on T) were long enough to assure that phase equilibrium was reached [7].

Heat-treated glasses were ground and analyzed using x-ray diffraction (XRD). Spinel mass fraction was determined from the area of a major peak between 0.256 nm and 0.245 nm d-spacing. The peak area, measured with Jade software, was calibrated using mixtures of spinel-free MS-7 glass and spinel isolated from a typical HLW glass [8].

The T_L values were calculated using previously published $T_{L,i}$ values [4]. To increase accuracy, Equation 3 was modified as follows

$$T_L = T_{BL} + \sum_{i=1}^{N} T_{L,i}(g_i - g_{Bi}) \quad (6)$$

where T_{BL} is the measured baseline glass T_L (1078°C) and g_{Bi} is the i-th component mass fraction in the baseline glass (Table I). Optical microscopy was used to confirm T_L in some glasses. Coefficients $C_{\max}$ and B_L were obtained using nonlinear least squares to fit Equation 1 to C_o data.

Values of a and n were measured in MS-7 and in the glasses with varying Al_2O_3, Cr_2O_3, Fe_2O_3, and NiO content. Optical microscopy was used to determine a, and XRD was used to determine C. Samples (2.6 g of glass) were first heated at 1200°C for 0.5 h; the

TABLE I Glass compositions in mass fractions

	Al_2O_3	B_2O_3	Cr_2O_3	Fe_2O_3	Li_2O	MgO	MnO	Na_2O	NiO	SiO_2	ZrO_2
MS-7	0.0800	0.0700	0.0030	0.1150	0.0454	0.0060	0.0050	0.1530	0.0095	0.4531	0.0600
H-Al	**0.1100**	0.0677	0.0029	0.1113	0.0439	0.0058	0.0048	0.1480	0.0092	0.4383	0.0580
L-Al	**0.0500**	0.0723	0.0031	0.1180	0.0469	0.0062	0.0052	0.1580	0.0098	0.4679	0.0620
H-Cr	0.0789	0.0699	**0.0050**	0.1148	0.0453	0.0060	0.0050	0.1527	0.0095	0.4522	0.0599
L-Cr	0.0802	0.0701	**0.0010**	0.1152	0.0455	0.0060	0.0050	0.1533	0.0095	0.4540	0.0601
H-Fe	0.0768	0.0672	0.0029	**0.1500**	0.0436	0.0058	0.0048	0.1469	0.0091	0.4352	0.0576
L-Fe	0.0832	0.0728	0.0031	**0.0800**	0.0472	0.0062	0.0052	0.1591	0.0099	0.4710	0.0624
H-Li	0.0788	0.0689	0.0030	0.1132	**0.0600**	0.0059	0.0049	0.1507	0.0094	0.4462	0.0591
L-Li	0.0813	0.0711	0.0030	0.1169	**0.0300**	0.0061	0.0051	0.1555	0.0097	0.4604	0.0610
H-Mg	0.0781	0.0683	0.0029	0.1122	0.0443	**0.0300**	0.0049	0.1493	0.0093	0.4422	0.0586
L-Mg	0.0805	0.0704	0.0030	0.1157	0.0457	**0.0000**	0.0050	0.1539	0.0096	0.4558	0.0604
H-Na	0.0774	0.0678	0.0029	0.1113	0.0440	0.0058	0.0048	**0.1800**	0.0092	0.4387	0.0581
L-Na	0.0831	0.0727	0.0031	0.1195	0.0472	0.0062	0.0052	**0.1200**	0.0099	0.4708	0.0623
VH-Ni	0.0783	0.0685	0.0029	0.1126	0.0445	0.0059	0.0049	0.1498	**0.0300**	0.4438	0.0588
H-Ni	0.0793	0.0694	0.0030	0.1140	0.0450	0.0059	0.0050	0.1517	**0.0180**	0.4492	0.0595
L-Ni	0.0805	0.0705	0.0030	0.1158	0.0457	0.0060	0.0050	0.1540	**0.0030**	0.4561	0.0604

temperature of the furnace was then reduced to 950°C and held for 5.5 h. This method was used to destroy nuclei before starting the heat treatment. Half of the sample was thin-sectioned and polished, and the other half was ground and analyzed using XRD. Transmitted light microscopy and image analysis software were used to determine a. C was determined as before from the area of the major peak. To calculate n densities for MS-7 and spinel were estimated as $\rho_g = 2.7$ mg/mm^3 and $\rho_s = 5.2$ mg/mm^3.

4. Results

Fig. 1 displays C_o, in mass fraction, as a function of $1/T$–$1/T_L$ to show the effect of glass composition on the spinel equilibrium fraction below T_L. The lines in Fig. 1 represent Equation 3 fitted to data. Note that, by Equation 3, $B_L C_{\max} = \mathrm{d}C_o(T \to T_L)/\mathrm{d}(1/T)$, i.e., the slope of the equilibrium curves at T_L. Table II lists and Fig. 2 displays T_L, $C_{\max}$, B_L, and ΔT values; the T_L was calculated using Equation 6, and the ΔT was calculated using Equation 4 with $C_o = 0.01$.

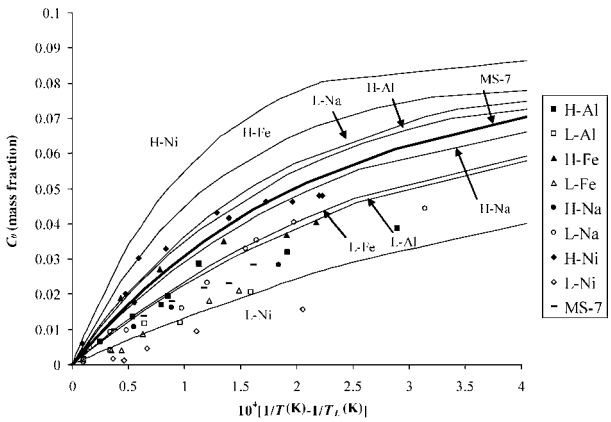

Figure 1 C_o versus $1/T$–$1/T_L$.

TABLE II Spinel equilibrium parameters

	$C_{\max}$	B_L (K)	T_L (°C)	ΔT (K)
MS-7	0.0828	4683	1078	30.0
H-Al	0.0828	5502	1136	28.5
L-Al	0.0819	3247	1018	39.0
H-Cr	0.0828	4683	1115	31.8
L-Cr	0.0828	4683	1039	27.1
H-Fe	0.0828	7816	1141	20.1
L-Fe	0.0819	3428	1015	36.7
H-Li	0.0828	3811	1042	34.4
L-Li	0.0828	3811	1117	39.5
H-Mg	0.0828	5320	1144	29.7
L-Mg	0.0828	4496	1062	30.3
H-Na	0.0819	4413	987	27.0
L-Na	0.0848	5638	1188	29.5
VH-Ni	0.1352	20282	1252	5.7
H-Ni	0.0927	9046	1151	15.8
L-Ni	0.0771	1894	1022	71.5

TABLE III Partial specific properties

	ΔT_i (K)	$C_{\max,i}$	$B_{L,i}$ (K)	$T_{L,i}$ (°C)
Al_2O_3	−121	0.096	38359	2848
Cr_2O_3	1212	0.090	8515	20578
Fe_2O_3	−176	0.094	60291	2670
Li_2O	−141	0.083	6502	−1333
MgO	−87	0.080	29871	2657
Na_2O	11	0.041	−12984	−1756
NiO	−3411	1.130	481053	9573
Remaining	166	0.073	−14201	1195
R^2	0.860	0.977	0.955	0.968

Partial specific values ($C_{\max,i}$, $B_{L,i}$, $T_{L,i}$, and ΔT_i) obtained by fitting Equation 5 to data (Table II) are displayed in Table III. The combined effects of components that were not varied (B_2O_3, MnO, SiO_2, and ZrO_2) are in the "Remaining" row.

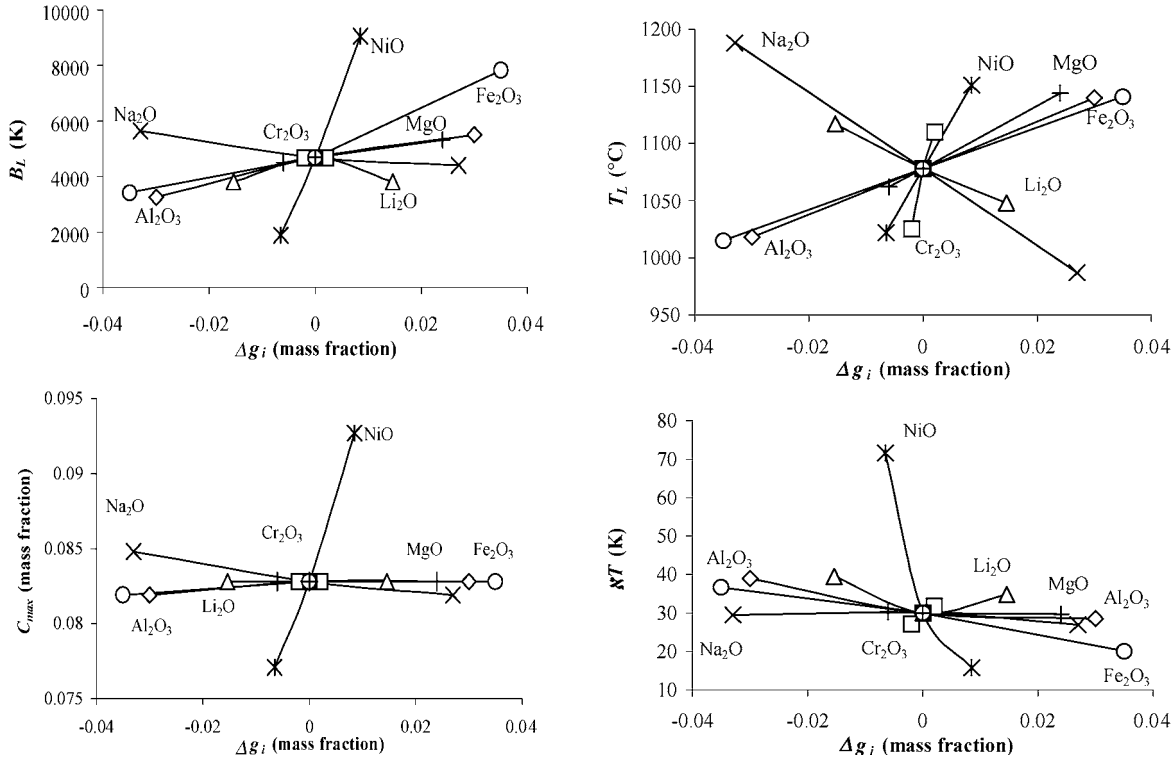

Figure 2 Effect of Δg_i on equilibrium parameters.

TABLE IV Crystal size and number density

	a (mm)	$\sigma^{(a)}$ (mm)	n (m^{-3})
MS-7	0.0486	0.0068	3.213E + 10
MS-7-L-Cr	0.0428	0.0071	1.096E + 10
MS-7-H-Cr	0.0502	0.0048	6.604E + 10
MS-7-L-Al	0.0387	0.0047	1.037E + 10
MS-7-H-Al	0.0484	0.0052	9.379E + 10
MS-7-L-Fe	0.0271	0.0032	1.888E + 10
MS-7-H-Fe	0.0660	0.0080	3.387E + 10
MS-7-L-Ni	0.0261	0.0024	3.211E + 10
MS-7-H-Ni	0.0697	0.0108	2.475E + 10

[a]σ is the standard deviation in crystal size.

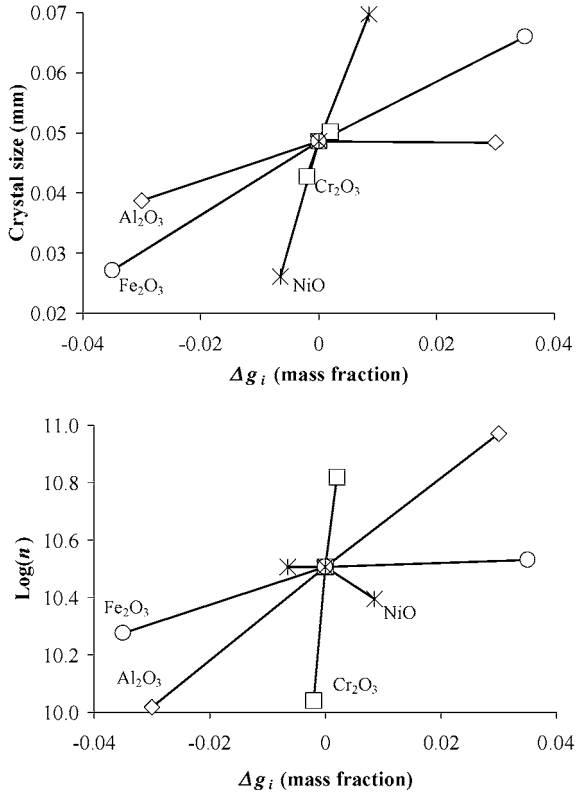

Figure 3 Effect of Δg_i on crystal size and number density of spinel crystals (in crystals per m^3).

Table IV lists and Fig. 3 displays the measured values of a and calculated values of n, obtained using the following equations:

$$V = \frac{1}{\left(\frac{1}{C} - 1\right)\frac{\rho_s}{\rho_g} + 1} \tag{7}$$

$$n = \frac{V}{a^3} \tag{8}$$

where V is the volume fraction of spinel, C is the mass fraction of spinel, ρ_g is the glass density, and ρ_s is the spinel density.

Because of the non-linear nature of n as a function of Δg_i, the partial specific property was calculated for log n (Table V). The combined effects of B_2O_3, Li_2O, MgO, MnO, Na_2O, SiO_2, and ZrO_2 are in the "Remaining" row.

5. Discussion

Nichromite ($NiCr_2O_4$) and trevorite ($NiFe_2O_4$) are two of the main three components of spinel found in MS-7 glass. Nichromite is the major spinel component of crystals that form near T_L whereas trevorite becomes the major spinel component together with magnetite (Fe_3O_4) as T approaches T_g (the glass-transition temperature). Not surprisingly, Ni has a drastic effect on both B_L and C_{max} and the second largest impact onT_L. Fig. 2 and Table III show that NiO has the largest impact on the ΔT. Removing the 0.01 mass fraction of NiO from baseline glass increases the ΔT by approximately 70°C, but adding NiO has a smaller effect, as seen in Fig. 2.

TABLE V Partial specific properties for a (in mm) and log n (n in m^{-3})

	a_i	$(\log n)_i$
Al_2O_3	0.485	11.153
Cr_2O_3	2.217	194.661
Fe_2O_3	0.838	−0.328
NiO	3.205	−11.391
Remaining	0.218	−6.025
R^2	0.989	0.985
R^2 Adjusted	0.971	0.960
Standard error	0.003	0.063

Fe also has an effect on spinel precipitation below T_L. The formation of magnetite at lower temperatures explains the substantial effect of Fe_2O_3 on C_{max}.

Cr had the greatest effect of any component on T_L; however, it had no measurable effect on either B_L or C_{max}. Despite Cr_2O_3's negligible effect on spinel precipitation below T_L, Cr still had one of the largest effects on ΔT because of ΔT's dependence on T_L—see Equation 4.

These results are comparable to those of Stachnik *et al.* [5], who studied the effects of Fe_2O_3, NiO, and Cr_2O_3 on spinel equilibrium in an HLW glass.

The addition of Na_2O and Li_2O reduced T_L, decreased C_{max} and B_L, and increased ΔT. Alkali ions interact with intermediate glass components such as Al and Fe, providing charge compensation to these components in their role as glass formers and providing them oxygen atoms to reach their appropriate coordination as glass modifiers. Thus, adding alkali oxides leads to an overall increase in the solubility of spinel-forming components and to an overall decline in the spinel content in glass.

Both MgO and Al_2O_3 increased T_L as much or more than Fe_2O_3, but had little impact on other parameters.

Fig. 3 shows that NiO, Cr_2O_3, and Fe_2O_3 increase a, whereas Al_2O_3 has little effect on a; Cr_2O_3 and Al_2O_3 increase n, while Fe_2O_3 and NiO have little effect on n. These results were obtained for $T = 950$°C. According to previous measurements [2], the log(n) decreases nearly linearly with T at $T > 800$°C (roughly, n decreases ten times when the temperature drops by 230°C), but no data exist regarding the relationship between n and the undercooling below T_L. Nevertheless, the strong impact of Cr_2O_3 on n as reflected by the large $\log(n)_i$ value in Table V is associated with the formation of Cr clusters in molten glass [11]. Spinel nucleates on these clusters. It is conceivable that Al promotes Cr cluster formation whereas Na reduces their occurrence.

6. Conclusion

Additions of Cr_2O_3 to glass increase T_L without significantly impacting the fraction of spinel in HLW glass. Additions of NiO increase T_L and drastically increase the spinel fraction in glass at T below T_L. These effects are augmented by additions of Fe_2O_3, Al_2O_3, and MgO and mitigated by additions of Na_2O and Li_2O. However, it may not be advantageous to decrease T_L by decreasing the content of Al_2O_3 and increasing the content of alkalis in glass because this would result in a lower chemical durability of the glass. Both Cr_2O_3 and Al_2O_3 increase crystal number density.

Acknowledgments

The authors would like to thank Brian Riley and Jose Rosario for help with XRD as well as Mike Schweiger and Jarrod Crum for help and advice in the laboratory. Ben Wilson is grateful to the Student Research Internship Program, Associated Western Universities, and Battelle for his appointment at Pacific Northwest National Laboratory. The Environmental Management Science Program of the U.S. Department of Energy provided funding for this task. Pacific Northwest National Laboratory is operated for the U.S. Department of Energy by Battelle under Contract DE-AC06-RL01830.

References

1. T. J. PLAISTED, F. MO, B. K. WILSON, C. YOUNG and P. HRMA, *Ceram. Trans.* **119** (2001) 317.
2. J. ALTON, T. J. PLAISTED and P. HRMA, *Chem. Engn. Sci.* **57** (2002) 2503.
3. M. W. STACHNIK, P. HRMA and H. LI, *Ceram. Trans.* **107** (2000) 123.
4. P. HRMA, J. D. VIENNA, J. V. CRUM, G. F. PIEPEL and M. MIKA, *Mat. Res. Proc.* **608** (2000) 671.
5. J. D. VIENNA, P. HRMA, J. V. CRUM and M. MIKA, *J. Non-cryst. Sol.* **292**(1–3) (2001) 1.
6. P. HRMA and J. D. VIENNA, *Ceram. Trans*. 2003 (in press).
7. J. G. REYNOLDS and P. HRMA, *Mat. Res. Proc.* **465** (1997) 65.
8. T. J. PLAISTED, J. ALTON, B. K. WILSON and P. HRMA, *Ceram. Trans.* **119** (2001) 291.
9. M. MIKA, M. PATEK, J. MAIXNER, S. RANDAKOVA and P. HRMA, in ICEM'01, The 8th International Conference On Radioactive Waste Management and Environmental Remediation, Bruges, Belgium (2001).
10. H. SCHOLZE, "Glass, Nature, Structure, and Properties" (Springer, New York, 1990).
11. J. G. DARAB, H. LI, D. W. MATSON, P. A. SMITH and R. K. MACCRONE, in "Synchrotron Radiation Techniques in Industrial, Chemical, and Materials Science," edited by K. L. D'Amico, L. J. Terminello and D. K. Shuh (Plenum, New York, 1996) p. 237.

Received 23 April 2001
and accepted 26 August 2002